Structural Engineering and Mechanics, *Vol. 65, No. 1 (2018) 43-51*
DOI: https://doi.org/10.12989/sem.2018.65.1.043

Analysis of thermal and damage effects over structural modal parameters

Fabricio A. Ortiz Morales[1], Alexandre A. Cury*[2] and Ricardo A. Fiorotti Peixoto[1]

[1]*Department of Civil Engineering, Federal University of Ouro Preto, Ouro Preto, MG, Brazil*
[2]*Department of Applied and Computational Mechanics, Federal University of Juiz de Fora, Juiz de Fora, MG, Brazil*

(Received April 2, 2017, Revised September 27, 2017, Accepted November 2, 2017)

Abstract. Structural modal parameters i.e. natural frequencies, damping ratios and mode shapes are dynamic features obtained either by measuring the vibration responses of a structure or by means of finite elements models. Over the past two decades, modal parameters have been used to detect damage in structures by observing its variations over time. However, such variations can also be caused by environmental factors such as humidity, wind and, more importantly, temperature. In so doing, the use of modal parameters as damage indicators can be seriously compromised if these effects are not properly tackled. Many researchers around the world have found numerous methods to mitigate the influence of such environmental factors from modal parameters and many advanced damage indicators have been developed and proposed to improve the reliability of structural health monitoring. In this paper, several vibration tests are performed on a simply supported steel beam subjected to different damage scenarios and temperature conditions, aiming to describe the variation in modal parameters due to temperature changes. Moreover, four statistical methodologies are proposed to identify damage. Results show a slightly linear decrease in the modal parameters due to temperature increase, although it is not possible to establish an empirical equation to describe this tendency.

Keywords: structural health monitoring; modal parameters; thermal effect; damage detection; structural dynamics

1. Introduction

Structural Health Monitoring (SHM) is based on the premise that damage cause changes in the structure's physical properties (stiffness, mass and damping). Over the last decades, modal parameters and other dynamic features obtained from vibration tests have been used to assess damage, since they are functions of such structural properties. Research in vibration-based damage identification has been rapidly expanding over the last few years, especially in applications involving bridges and buildings. In their survey, Mohan *et al*. (2014) have developed a correlation-based approach between vectors of experimental natural frequency change ratios with vectors of analytical natural frequency change ratios. More recently, Wang *et al*. (2016) have proposed a novel concept, combining information from frequency shifting and amplitude changing for damage detection. However, modal parameters are also sensitive to environmental factors such as humidity, wind and temperature. The latter is especially responsible for modal variations that often are higher than those caused by structural damage. This condition might compromise the reliability of SHM techniques, by either masking the presence of damage or giving false positive alarms. To overcome this problem, many researchers have studied the underlying relationships between modal parameters, environmental factors and structural damage. Such studies were performed by means of numerical simulations and experimental tests in laboratory or in situ, as described in references Farrar *et al.* (1994), Farrar *et al.* (1997), Alampalli (1998), Rohrmann *et al.* (2000), Peeters *et al.* (2001), Sohn *et al.* (1999), Meruane and Heylen (2012), Cury *et al.* (2011), Nguyen *et al.* (2014), Ling (2015), Wei (2015).

Moreover, many damage identification techniques and algorithms have been proposed and used for the statistical discrimination of damage, such as: linear regressions based on neural networks and linear adaptive filters (Sohn *et al*. 1999) and more recently, Saisi *et al*. (2015), Gentile *et al*. (2016) have assessed the effects of changing temperature on the natural frequencies of a historic tower; ARX models (Peeters *et al*. 2001); modal assurance criterion MAC (Allemang 2002); principal component analysis and novelty index (Yan *et al*. 2005a, b); hypothesis tests (Chinmaya and Mohanty 2006); symbolic data analysis with clustering techniques and novelty index (Alves *et al*. 2015, Alves *et al*. 2016); optimized detection based on parallel genetic algorithms (Xu 2015), among others. Despite many authors have found empirical equations through the correlation of natural frequencies and temperature using either simple, complex, traditional or novelty techniques, no generalized empirical equation has ever been found. In other words, there is no law that clearly describes the relationship between modal parameters and temperature, which allows distinguishing variations due to damage from those due to temperature changes.

To provide a better understanding over such a phenomenon, this paper proposes an experimental study of the variation of modal parameter estimates due to temperature and damage. This study is performed on a simply supported steel beam subjected to 20 different temperature setups and 3 structural damage scenarios,

*Corresponding author, Professor
E-mail: alexandre.cury@ufjf.edu.br

http://www.techno-press.com/journals/sem&subpage=7
ISSN: 1225-4568 (Print), 1598-6217 (Online)

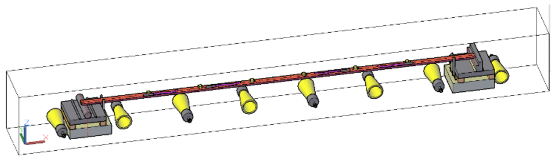

Fig. 1 General scheme of the experiment

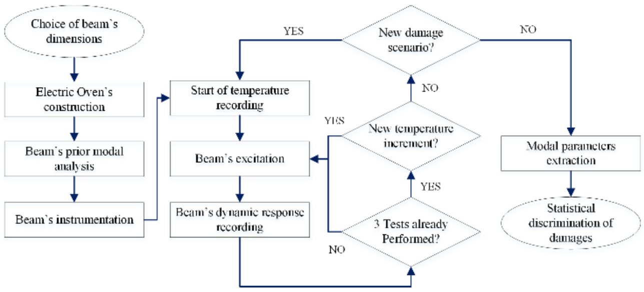

Fig. 2 Methodology's flowchart

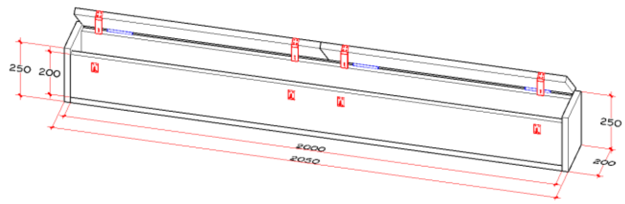

Fig. 3 Nominal dimensions in mm of the electric oven

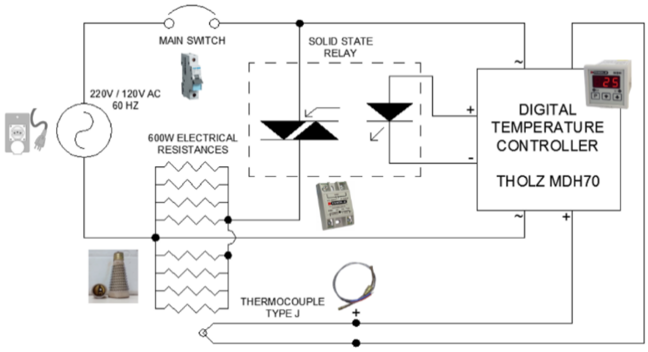

Fig. 4 Oven's schematic electric diagram

yielding 180 tests. To assess these three damage scenarios under the effect of temperature variation, four statistical damage detection techniques are proposed: confidence intervals, robust linear regression, control charts and hypothesis tests. Results show that among the four proposed techniques, only one is reliable for structural damage detection.

2. Materials and methods

The methodology proposed in this paper consists in placing a steel beam into an electric oven and heating it up progressively while performing vibration tests under different temperatures and damage conditions. Is important to observe that this methodology is in accordance with the Structural Health Monitoring Process as suggested by Los Alamos National Laboratory (LANL) in the report LA13976-MS and by Farrar (2013). Fig. 1 depicts the general scheme of the experiment and Fig. 2 shows the flowchart of the proposed methodology.

An A36 steel flat bar with nominal dimensions of 25 mm×6 mm×1500 mm was chosen to the tests, since such dimensions yield rather low natural frequencies as those observed in many large civil engineering structures.

It is important to note that the boundary conditions remained unchanged throughout the tests, allowing the beam's natural thermal expansion, as Fig. 1 shows. Moreover, there is no relative displacement between the box and the supports. The beam was slightly glued to the supports to avoid vertical displacements. The longitudinal displacements are allowed, since the cylinder above the left support is not fixed (contrary to the right support). Even though the beam is considered isostatic, which is not always the case for real civil structures, the results obtained should provide useful insights about the general relationships between modal parameters and temperature.

2.1 Electrical oven construction

Before performing the vibration tests, it was necessary to build an electric oven, which consists in a parallelepiped timber box with external dimensions of 200 mm×250 mm×2050 mm (Fig. 3). To minimize heat losses, were used an internal ceramic sheathing and a polyethylene foam-sealing strip to fill the gaps between the openings and the oven's box.

Eight electrical resistances of 600 W uniformly distributed along the oven's length served as sources of heat. A J-type thermocouple, a solid-state relay and a digital temperature controller composed the power controlling system. Fig. 4 shows the oven's schematic electric diagram. More details about the design, construction process and operation can be found in Ortiz (2016).

2.2 Experimental setting and beam's previous analysis.

The minimum temperature for all tests was set to 18°C, since it was the minimum temperature reachable using an air conditioning system. The maximum temperature for all tests was 56°C. This maximum temperature was set to: i) do not damage the insulation of the accelerometer's coaxial cables (for which safe operational temperature must be under 70°C); ii) obtain an adequate sampling of readings (20 samples obtained at intervals of 2°C); iii) obtain a temperature gradient of 38°C which is wider than seasonal temperature variation in many tropical countries.

After choosing the lower and upper temperatures values for the experiment, a prior modal analysis of the beam was performed to assess its natural frequencies and its possible changes due to thermal and damage effects. Eq. (1) yields the natural frequencies for a simply supported beam. Table 1 shows the natural frequencies for the first three bending modes.

$$f_i = \frac{i^2 \times \pi}{2} \times \sqrt{\frac{E \times I}{\rho \times A \times L^4}} \quad (1)$$

Table 1 Natural frequencies of the bending modes for the undamaged scenario at room temperature (25°C)

Bending mode	Frequency [Hz]
First	6.00
Second	24.00
Third	54.01

Table 2 Theoretical values of the undamaged natural frequencies for the minimum and maximum temperatures

Bending mode	Frequency at 18°C [Hz]	Frequency at 56°C [Hz]	ΔFrequency [Hz]
First	6.00	5.97	-0.03
Second	24.02	23.89	-0.13
Third	54.01	53.77	-0.29

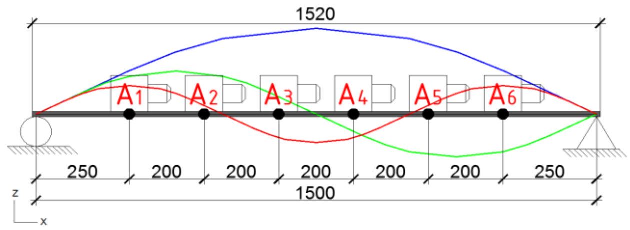

Fig. 5 Accelerometers' instrumentation scheme (dimensions in mm)

i:1st, 2nd, 3rd bending modes
f_i: frequency in Hz
E: Steel Young's modulus at 25°C 200e9 Pa
I: moment of inertia 429.58e-12 m^4
ρ: material density 7850 kg/m^3
A: cross section area 148.09e-6 m^2
L: free span 1.50 m

Moreover, Eq. (2) is used to estimate the thermal effects over the natural frequencies, by evaluating the Young's modulus E according to the temperature (Poh 2001). Table 2 presents the expected natural frequencies for the minimum and maximum temperatures for an undamaged scenario.

$$E_0 \left[1 + \frac{T}{c_9 \ ln\left(\frac{T}{c_{10}}\right)} \right] \quad \text{for} \quad 0°C < T \leq 600°C \qquad (2)$$

E_0: Steel Young's modulus estimated at 0°C (201.04 GPa)
T: temperature in °C
c_9: coefficient equal to 1100
c_{10}: coefficient equal to 2000

2.3 Beam's instrumentation

The beam's dynamic responses were measured using six unidirectional piezoelectric accelerometers Brüel and Kjaer 4507B series with sensitivity of 10 mV/g and frequency range of 0.3 Hz to 6 kHz. Fig. 5 shows the instrumentation scheme.

Moreover, four temperature sensors were used (TCM-HD50 series), which have an operational range from -40°C to 100°C and an accuracy of 0.25°C. Fig. 6 depicts the sensor's instrumentation scheme. A global view of the beam's instrumentation is shown in Fig. 7.

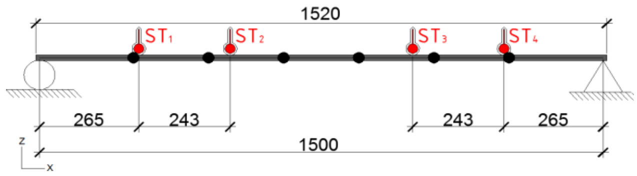

Fig. 6 Temperature sensors' placement scheme

Fig. 7 Beam's instrumentation scheme

Table 3 Vibration tests acquisition parameters

Parameter	Value
Sampling time	15s
Sampling rate	1000 Hz
Low pass filter	100 Hz
Gain	2x

2.4 Dynamic tests

Dynamic tests were carried out by means of forced vibrations, which consisted in applying a 15 mm vertical displacement through a quasi-static force and then releasing it abruptly. The displacement was applied at 260 mm from the left support to provide a better identification of the first three bending modes.

The beam's accelerations were recorded using a signal recorder/conditioner Lynx ADS 2000, which has a 16-bit resolution A/D converter. The acquisition parameters are summarized in Table 3.

The beam's modal parameters were extracted using an automated SSI-DATA (Stochastic Subspace Identification) algorithm developed by Cardoso (2017).

2.5 Temperature recording

Temperature values were recorded at one-second interval using a Hoboware® U12 series data logger. At every 5 minutes, approximately, the temperature was incremented by 2°C. Three vibration tests were performed at each temperature. Fig. 8 shows a typical temperature record history. The R^2 coefficient demonstrate that those increments follow a linear path.

2.6 Damage scenarios

Artificial damage scenarios were simulated by cutting the beam's cross section to change local stiffness and cause a reduction in the natural frequencies. Fig. 9 details the two damage scenarios. The first one reduces the beam's cross

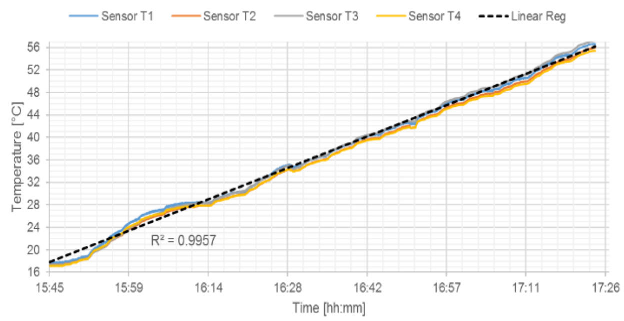

Fig. 8 Incremental temperature path

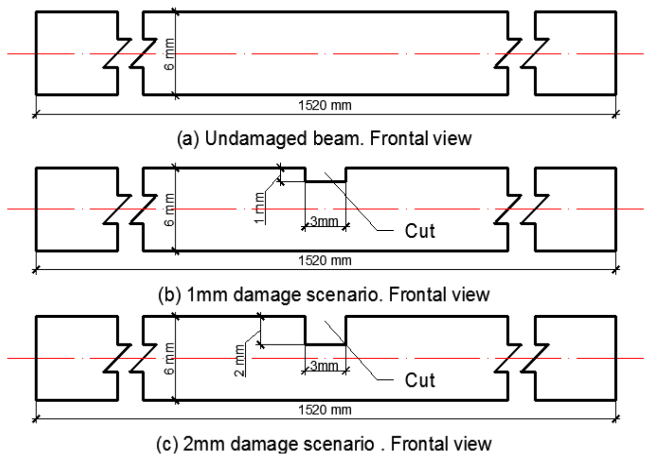

Fig. 9 Beam's damage scenarios simulated through electrical saw cuts

section area by 16.67% whereas the second by 33.34%.

2.7 Statistical methods for damage detection

The proposed techniques aim to identify damage through statistical analyses of the vibration features identified by the modal analysis. The main idea is to detect structural damage by means of natural frequency deviations under thermal effects. Four methods are proposed: analysis of confidence intervals, robust linear regressions, control charts and hypothesis tests.

2.7.1 Confidence intervals

A confidence interval gives an estimated range of values that is likely to include an unknown population parameter. The estimated range is calculated from a given set of sample data. This analysis looks for some keys patterns of the natural frequencies behavior affected by temperature changes and structural damage. To this end, mean values and standard deviations of the natural frequencies estimates are evaluated for every temperature reading and for all damage scenarios. In this study, one considers 95% confidence intervals (equivalent to $m \pm 1.96\sigma$, where m is the mean value and σ is the standard deviation of the frequencies' estimates).

2.7.2 Robust linear regressions

This method is based on an iterative reweighted least squares method, which is less sensitive to outliers compared to traditional linear regressions methodologies. Eq. (3) summarizes the robust linear regression method used in this paper. More details about this method can be found in Hastie (2009).

$$\beta^{(t+1)} = argmin_{\beta}(\boldsymbol{z} - \boldsymbol{X}\beta)^T \boldsymbol{W}(\boldsymbol{z} - \boldsymbol{X}\beta) \qquad (3)$$

where:

$argmin_{\beta}$: is a minimum of β, i.e., the derivative of the expression with respect to β, then equals to zero and solve for β

$\beta^{(t+1)}$: Coefficients vector of the new iteration

$\boldsymbol{z}$: $\mathbf{X}\beta + \boldsymbol{W}^{-1}(\boldsymbol{Y} - \boldsymbol{P})$, where:

$\boldsymbol{W}$: diagonal matrix N x N which contains the i-th diagonal element $p(x_i;\beta)(1 - p(x_i;\beta))$

$\boldsymbol{P}$: adjusted probabilities vector with i-th element $p(x_i;\beta)$

$\boldsymbol{Y}$: vector of natural frequencies y_i

X: vector of temperatures x_i

β: vector of coefficients $\beta_0, \beta_1, \dots, \beta_p$

2.7.3 Control charts

This methodology was first used for the quality control in the manufacturing industry, aiming the detection of abnormalities in their processes. A control chart is a time series graph composed by a central line, and two (upper and lower) bounds usually called control bounds, which are calculated from data dispersion of a reference state in the process being monitored. This methodology assumes that the intrinsic variations of a process are normally distributed. The control bounds set a confidence interval of $\pm 3\sigma$, which means that exist a 99.73% of probability that all data are within this interval.

When some data fall outside the bounds, it indicates the occurrence of abnormalities, probably due to external factors (Oakland 2007). There are many types of control charts, but in this paper, the *X*-type control chart was used, since it monitors the mean value of the frequencies for all temperature conditions and damage scenarios. The control bounds were calculated using Eqs. (4) and (5) considering the undamaged scenario as the reference state and a confidence interval of 95% ($\pm 1.96\sigma$).

$$Control\ bounds = \mu_{\bar{x}} \pm 1{,}96\sigma_{\bar{x}} \qquad (4)$$

$$\sigma_{\bar{x}} = \frac{\sigma}{\sqrt{n}} \qquad (5)$$

where:

$\mu_{\bar{x}}$: mean of the reference state

$\sigma_{\bar{x}}$: standard deviation of the subgroups in the reference state

σ: standard deviation of the reference state

n: subgroups size of the reference state

2.7.4 Kolgomorov–Smirnov Hypothesis test

The Kolgomov-Smirnov test is a nonparametric hypothesis test that returns a decision on whether two data sets have the same probability distribution (*H*=0 if true or *H*=1 if false). The decision is based on the statistic *D*-stat calculated using Eq. (6), which represents the maximum absolute difference between the Empirical Cumulative

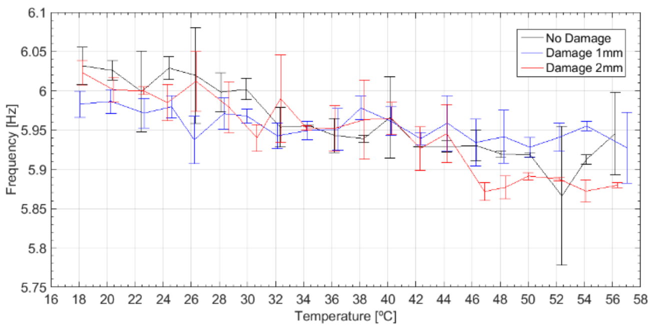

Fig. 10 First frequency mean values and confidence intervals of all damage scenarios

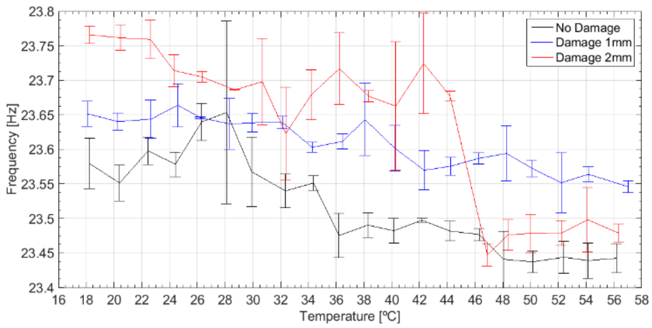

Fig. 11 Second frequency mean values and confidence intervals for all damage scenarios

Distribution Functions (ECDF) of the two data sets compared. Moreover, the test provides the parameter *p*-value, which is the probability of the null hypothesis being true, even if the test rejects the null hypothesis. More details about the Kolgomorov-Smirnov Test and interpretation of the p-value can be found in Chinmaya and Mohanty (2006), Mathworks Inc (2015), Wasserstein and Lazar (2016).

$$D_{stat} = |F_0(x) - F(x)| \qquad (6)$$

where:

D_{stat}: maximum absolute difference between $F_0(x)$ and $F(x)$.

$F_0(x)$: cumulative distribution function of the first data set.

$F(x)$: cumulative distribution function of the second data set.

In this paper, the KS test was used to answer the following questions:

1) Do natural frequencies variations follow a normal distribution?

2) If not, do natural frequencies variations follow the same non-Gaussian distribution?

The test was also used as a damage indicator through the D-stat values. To this end, one compares the data sets containing the 1st, 2nd and 3rd natural frequencies of the 3 damage scenarios and observes the continuous variation of D-stat values. In other words, one considers three vectors $f$id0, $f$id1, $f$id2, which contains the 20 mean values of the natural frequencies of the *i*-th vibration mode obtained for the 3 damage scenarios (d0, d1 and d2) and for the 20 temperature sets. If one compares the vectors of the 1st natural frequency of the undamaged scenario (f1d0) with the 1st natural frequency of the 1mm damage scenario (f1d1), it is expected that both ECDF are different. In fact, since damage reduces structure's stiffness, natural frequencies of the 1 mm damage scenario will be smaller than those of the undamaged scenario. Consequently, the shape of both ECDF will be different. This difference is indicated through the statistic D-stat. Thus, a continuous variation of this number is an indicator that damage is being identified between successive datasets. It is important to notice that structural damage is the unique source of variability in this experiment, since all the natural frequencies in all damage scenarios were obtained approximately at the same temperatures, excitation and boundary conditions.

3. Results and discussion

The following sections present the results obtained by the four proposed statistical damage detection techniques applied to 180 vibration tests performed on the beam (3 tests at 20 temperatures under 3 damage scenarios). The first results correspond to the analysis of frequencies estimates at different temperatures. In fact, one analyzes how the mean values and confidence intervals vary according to damage and temperature evolution. Then, robust linear regression as well as control chart analyses are performed. Finally, one investigates the results obtained by Kolgomorov-Smirnov hypothesis tests.

3.1 Mean-values analysis

Figs. 10, 11 and 12 show the mean values and a 95% confidence interval for the three natural frequencies estimates obtained from three vibration tests performed at different temperatures and for all damage scenarios. In general, one observes that the frequencies tend to decrease when the temperature rises (as expected). However, this pattern is not purely linear. Moreover, one notices that the estimated frequencies are slightly higher than those calculated analytically are (see Table 2).

For the case of the first natural frequency (Fig. 10), one observes that is possible to identify a reduction due to the presence of damage. However, the confidence intervals overlap all over the estimates, making it statistically impossible to assert the existence of damage.

Fig. 11 shows the mean values and confidence intervals for the second natural frequency. It is possible to notice that for many of the estimates, the confidence intervals do not overlap, which would statistically allow identifying the different damage scenarios. However, some estimates present an erratic behavior. This could be because the artificial damage is located at the middle of the span, which is an inflexion point for the second bending mode, thus yielding poor damage estimates for the second natural frequency.

Fig. 12 displays the same analysis for the third natural frequency. Note that tendencies do not show a clear relationship between frequencies and temperature. In addition, it is not possible to identify statistically the damage scenarios, since the confidence intervals overlap for almost all estimates.

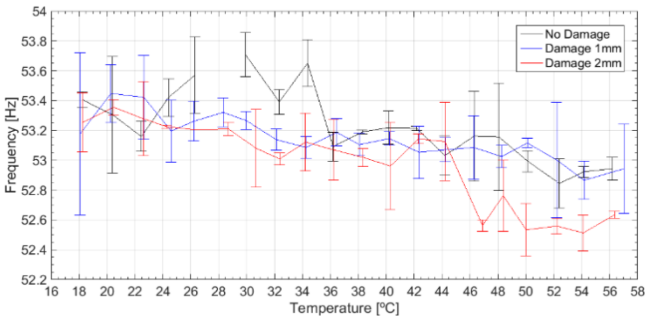

Fig. 12 Third frequency mean values and confidence intervals for all damage scenarios

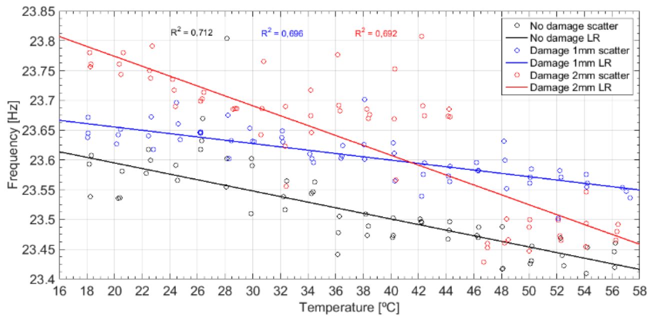

Fig. 14 Scatter plot and robust linear regression of the second frequency for all damage scenarios

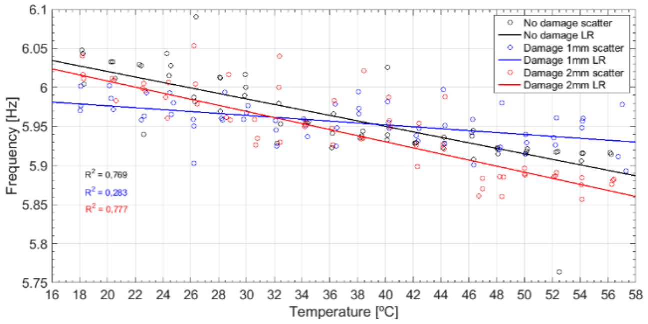

Fig. 13 Scatter plot and robust linear regression of the first frequency for all damage scenarios

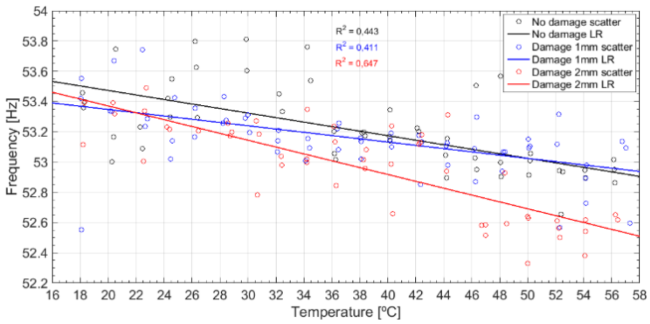

Fig. 15 Scatter plot and robust linear regression of the third frequency for all damage scenarios

3.2 Robust linear regressions analyses

Figs. 13 to 15 show the scatter plots and the robust linear regression models for each natural frequency. In general, one observes that the natural frequencies decrease linearly when the temperature rises. Fig. 13 shows the results for first natural frequency for all damage scenarios. Note that linear regressions of the undamaged scenario and 2 mm damage scenario have almost the same slope, which indicate that the frequency decrease at the same rate when the temperature rises. In addition, one notices that frequency estimates for the 2 mm damage scenario are lower than those of the undamaged scenario (as expected). Moreover, the coefficient of determination (R^2) of both linear regressions are similar, which indicate that both models fit the datasets similarly. However, the linear regression for the 1mm damage scenario appears to be less affected by temperature, since its slope is smaller than the others. Moreover, for the temperatures between 40°C and 56°C, the frequencies are higher than those identified in the undamaged scenario. This difference could be explained by the low value of R^2, which means that the linear regression for the 1mm damage scenario does not represent its behavior properly.

From the linear regression for the second natural frequencies, it is possible to identify all damage scenarios (see Fig. 14). Moreover, the coefficients of determination (R^2) for the three linear regression models are similar, which means that the models fit the datasets very similarly. Once again, one observes some erratic estimates possibly caused by the reasons previously explained.

Fig. 15 shows the linear regression models for the third natural frequency. In this case, all damage scenarios are distinguishable. The values of the coefficients of determination are lower than those computed for the first and second natural frequencies. This fact is due to the higher dispersion of the estimates, since higher modes are more difficult to identify with precision.

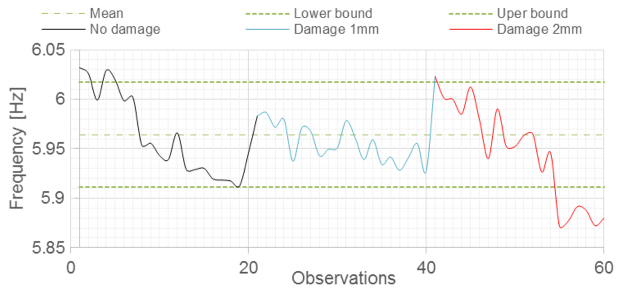

Fig. 16 Control chart of the first frequency for all damage scenarios

3.3 Control charts analyses

In these analyses, the control limits are calculated using the "no damage" scenario as reference state. Then, the other two damage scenarios are plotted as a time series to identify the presence of outliers.

In Fig. 16, the control chart of the first natural frequency for all damage scenarios shows that some outliers were identified only for the 2 mm damage scenario for temperatures above 44°C. Once again, one notices that the first damage scenario (in blue) seems to be less affected by the temperature, since this dataset shows less variation than the reference state (in black).

The existence of some outliers in the undamaged

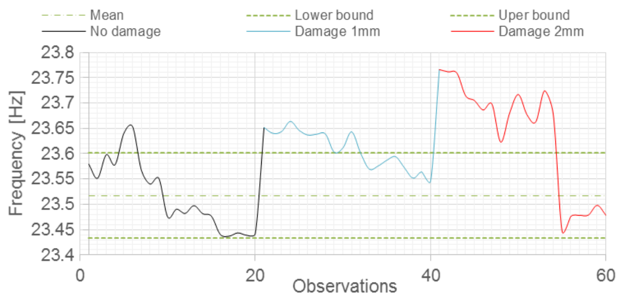

Fig. 17 Control chart of the second frequency for all damage scenarios

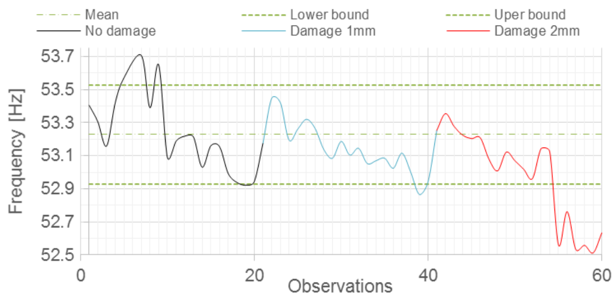

Fig. 18 Control chart of the third frequency for all damage scenarios

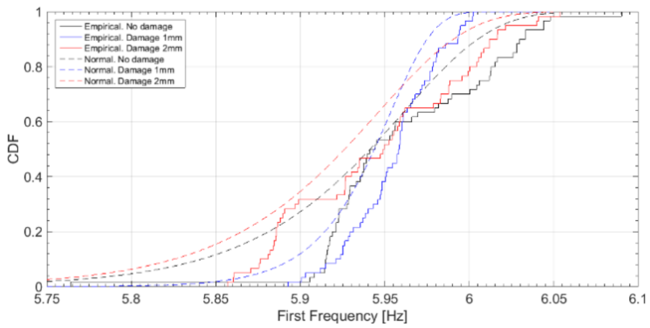

Fig. 19 Comparison of the empirical and normal cumulative distribution frequencies of the first natural frequencies for all damage scenarios

scenario could be explained as: i) those outliers represent the 5% uncertainty of the methodology; ii) the data does not follow a normal distribution. This last hypothesis is further tested using the Kolmogorov-Smirnov test.

Fig. 17 presents the results for the second natural frequency. Again, the estimates tend to increase with the presence of damage. However, even though many values fall above the upper limit, one cannot state that damage was correctly identified, since the presence of damage should be detected as outliers below the lower limit.

Fig. 18 shows the control chart for the third natural frequency. It is possible to identify one outlier in the 1mm damage scenario (in blue) and six outliers in the second damage scenario (in red) for temperatures above 44°C. Notice that even in the reference state (undamaged scenario) there are outliers above the upper limit. However, as previously stated, only the lower limit matters, since the basic premise stablishes that damage reduces the natural frequencies.

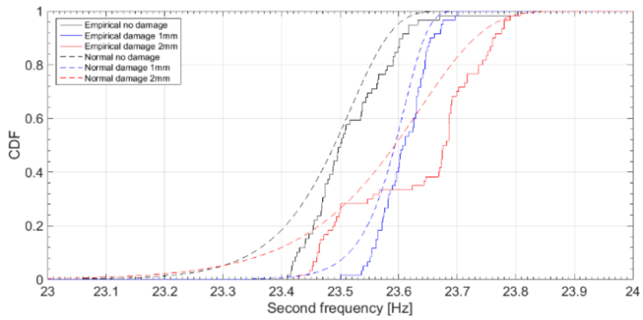

Fig. 20 Comparison of the empirical and normal cumulative distribution frequencies of the second natural frequencies for all damage scenarios

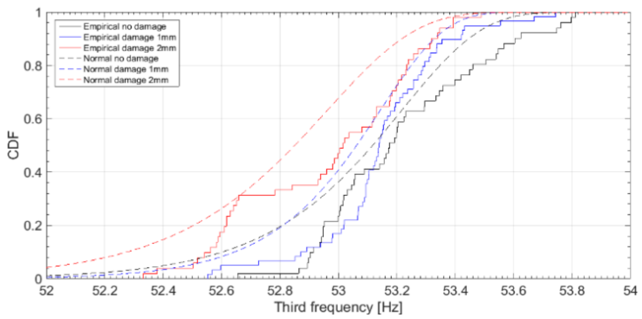

Fig. 21 Comparison of the empirical and normal cumulative distribution frequencies of the third natural frequencies for all damage scenarios

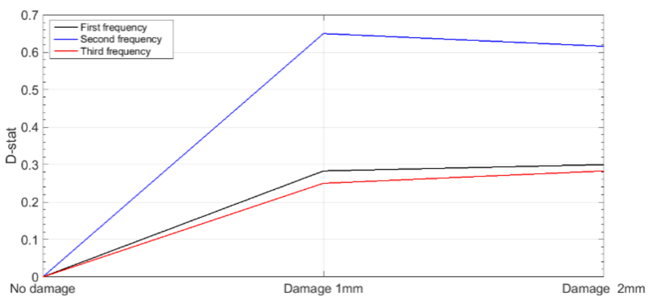

Fig. 22 *D*-stat values for the three frequencies and all damage scenarios

3.4 Kolgomorov-Smirnov Hypothesis tests

The following tables and figures show the results obtained through the Kolgomorov-Smirnov hypothesis tests. For all datasets, two hypotheses were tested: i) do the data follow a normal distribution? ii) if not, do the data follow the same non Gaussian distribution?

The results for the first hypothesis are shown in Table 4. The results show that not all datasets follow a normal distribution. This can be observed in Figs. 19 to 21, where the first three natural frequencies for all damage scenarios are compared with the normal distribution curves of the datasets.

Table 5 shows the results for the second hypothesis. By observing the *H* values, it is clear that not all datasets follow the same non Gaussian distribution, i.e., each dataset follows its own frequency distribution. Since the temperature is a controlled variable in this study, the unique

Table 4 First hypothesis testing values for all natural frequencies and all damage scenarios

	f1d0	f1d1	f1d2	f2d0	f2d1	f2d2	f3d0	f3d1	f3d2
D-stat	1	1	1	0.983	1	1	0.850	0.983	0.850
p-value	0	0	0	0	0	0	0	0	0
H	**1**	**1**	**1**	**1**	**1**	**1**	**1**	**1**	**1**

f: natural frequency in Hz; *d**: damage level; *D*-stat: absolute maximum difference; *H*: decision value based on 95% confidence bounds, returning 0 if null hypothesis is true and 1 if false; *p*-value: null hypothesis probability.

Table 5 Second hypothesis testing values for all natural frequencies and all damage scenarios.

		f1d0	f1d1	f1d2	f2d0	f2d1	f2d2	f3d0	f3d1	f3d2
	D-stat	**0**	**0.283**	**0.300**						
f1d0	p-value	1	0.012	0.006						
	H	0	1	1						
	D-stat				**0**	**0.650**	**0.616**			
f2d0	p-value				1	0	0			
	H				0	1	1			
	D-stat							**0**	**0.250**	**0.283**
f3d0	p-value							1	0.038	0.012
	H							0	1	1

f: natural frequency in Hz; *d**: damage level; *D*-stat: absolute maximum difference; *H*: decision value based on 95% confidence bounds, returning 0 if null hypothesis is true and 1 if false; *p*-value: null hypothesis probability

source of variability is damage. Thus, one may suppose that the *D*-stat values (characters in italic in Table 5) could be used as damage indicators. Fig. 22 shows that the Kolmogorov-Smirnov Test identified successfully all damage scenarios, since its values are always increasing between datasets.

4. Conclusions

Table 6 provides a qualitative summary of the results obtained by the proposed techniques used in this paper. This summary is based on the answer of two main questions:

1. Did the method reveal a clear relationship between natural frequencies, temperature and damage?
2. Did the method successfully identify all damage scenarios?

In general, mean values and confidence intervals did not successfully identify any clear relationship between natural frequencies, temperature and damage.

Scatter plot and linear regressions showed a clear relationship between damage, temperature and natural frequencies, but in some cases, the models did not fit well the entire dataset. Thus, this method partially identified the damage scenarios and showed a limited relationship between those physical quantities.

Control charts did not identify the damage scenarios properly. This could be because control charts methodology considers that data are normally distributed, which was not the case.

Table 6 Summary of the results obtained through all the methods

Method	Question 1	Question 2
Mean values	No	No
Robust linear regression	Partially	Partially
Control charts	No	Partially
Kolmogorov hypothesis test	Not applicable	Yes

Kolmogorov-Smirnov Hypothesis Tests showed to be effective in damage detection, taking as premise that the unique source of variability in this experiment was damage.

Finally, it was impossible to establish an empirical equation that describes the relationship between natural frequencies, temperature and damage due to the complexity of this phenomenon.

Acknowledgments

This work has been supported by the Organization of American States OAS, Coimbra Group of Brazilian Universities GCUB, CNPq (National Council for Scientific and Technological Development), FAPEMIG (Foundation of Support Research of the State of Minas Gerais), CAPES (Coordination for the Improvement of Higher Education Personnel). The authors also thank RECICLOS (Research Group UFOP), which provided the physical space to perform this research.

References

Alampalli, S. (1998), "Influence of in-service environment on modal parameters", *Proceedings IMAC XVI-International Modal Analysis Conference*, 111-116.

Allemang, R.J. (2002), "The Modal Assurance Criterion (MAC): Twenty years of use and abuse", *Proceedings IMAC XX-International Modal Analysis Conference.*

Alves, V., Cury, A. and Cremona, C. (2016), "On the use of symbolic vibration data for robust structural health monitoring", *Proc. Inst. Civil Eng. Struct. Build.*, **169**(9), 715-723.

Alves, V., Cury, A., Roitman, N., Magluta, C. and Cremona, C. (2015), "Novelty detection for SHM using raw acceleration measurements", *Struct. Control Hlth. Monit.*, **22**(9), 1193-1207.

Cardoso, R., Cury, A. and Barbosa, F. (2017), "A robust methodology for modal parameters estimation applied to SHM", *Mech. Syst. Signal Pr.*, **95**, 24-41.

Chinmaya, K. and Mohanty, A.R. (2006), "Multistage gearbox condition monitoring using motor current signature analysis and Kolgomorov-Smirnov test", *J. Sound Vib.*, **290**, 337-368.

Cury, A.A., Borges, C.C.H. and Barbosa, F.S. (2011), "A two-step technique for damage assessment using numerical and experimental vibration data", *Struct. Hlth. Monit.*, **10**(4), 417-428.

Farrar, C.R. and Worden, K. (2013), *Structural Health Monitoring: A Machine Learning Perspective,* John Wiley & Sons.

Farrar, C.R., Baker, W.E., Bell, T.M., Cone, K.M., Darling, T.W., Duffey, T.A., ... and Migliori, A. (1994). "Dynamic characterization and damage detection in the I-40 bridge over the Rio Grande (No. LA--12767-MS)", Los Alamos National Lab., NM, USA.

Farrar, C.R., Doebling, S.W., Cornwell, P.J. and Straser, E.G. (1997), "Variability of modal parameters measured on the Alamosa Canyon Bridge", *Proceedings IMAC XV-International Modal Analysis Conference.*

Gentile C., Guidobaldi, M. and Saisi, A. (2016), "One-year dynamic monitoring of a historic tower: damage detection under changing environment", *Meccanica*, **51**(11), 2873-2889.

Hastie (2009), *The Elements of Statistical Learning: Data Mining, Inference and Prediction*, 2nd Edition, Palo Alto, California: Springer.

Mathwoks Inc. (2015), "Kolmogorov test/Documentation Center/ Statistical Toolbox", http://www.mathworks.com.

Meruane, V. and Heylen, W. (2012), "Structural damage assessment under varying temperature conditions", *Struct. Hlth. Monit.*, **11**, 345-357.

Nguyen, V.H., Mahowald, J., Golinval, J.C. and Maas, S. (2014), "Damage detection in bridge structures including environmental effects", *Proceedings of the 9th International Conference on Structural Dynamics*, EURODYN.

Oakland, J. (2007), *Statistical Process Control*, 6th Edition, Routledge.

Ortiz Morales, F.A. (2016), "Avaliação da influência da temperatura sobre os parâmetros modais de estruturas", Dissertação de mestrado. Universidade Federal de Ouro Preto, Ouro Preto.

Peeters, B. and De Roeck, G. (2001), "One-year monitoring of the Z-24 Bridge: Environmental effects vs damage events", *Earthq. Eng. Struct. Dyn.*, **30**, 149-171.

Poh, W. (2001), "Stress-strain-temperature relationship for structural steel", *J. Mater. Civil Eng.*, **13**(5), 371-379.

Rohrmann, R.G., Baessler, M., Said, S. and Schmid, W. (2000), "Structural causes of temperature affected modal data of civil structures obtained by long time monitoring", *Proceedings IMAC XVIII-International Modal Analysis Conference*, 1-7.

Saisi, A., Gentile, C. and Guidobaldi, M. (2015), "Post-earthquake continuous dynamic monitoring of the Gabbia Tower in Mantua, Italy", *Constr. Build. Mater.*, **81**, 101-112.

Sohn, H., Dzwonczyk, M., Straser, E.G., Kiremidjian, A.S., Law, K.H. and Meng, T. (1999), "An experimental study of temperature effect on modal parameters of the Alamosa Canyon Bridge", *Earthq. Eng. Struct. Dyn.*, **28**, 879-897.

Soon, H., Farrar, C.R., Hemez, F.M., Shunk, D.D., Stinemates, D.W. and Nadler, B.R. (2004), "A review of structural health monitoring literature", Report LA13976MS, 1996-2001.

Vimal Mohan, S., Parivallal, K., Kesavan, B., Arunsundaram, A., Farvaze Ahmed, K. and Ravisankar, K. (2014), "Studies on damage detection using frequency change correlation approach for health assessment", *Procedia Eng.*, **86**, 503-510.

Wang, L., Lie, S.T. and Zhang, Y. (2016), "Damage detection using frequency shift path", *Mech. Syst. Signal Pr.*, **66-67**, 298-313.

Wasserstein, R. and Lazar, N.A. (2016), "The ASA's statement on p-values: context, process and purpose", *Am. Statistic.*, **70**(2), 129-133.

Wei, J.J. and Lv, Z.R. (2015), "Structural damage detection including the temperature difference based on response sensitivity analysis", *Struct. Eng. Mech.*, **53**(2), 249-260.

Xu, H.J., Ding, Z.H., Lu, Z.R. and Liu, J.K. (2015), "Structural damage detection based on Chaotic Artificial Bee Colony algorithm", *Struct. Eng. Mech.*, **55**(6), 1223-1239.

Yan, A.M., Kerschen, G., De Boe, P. and Golinval, J.C. (2005a), "Structural damage diagnosis under varying environmental conditions-part I: A linear analysis", *Mech. Syst. Signal Pr.*, **19**, 847-864.

Yan, A.M., Kerschen, G., De Boe, P. and Golinval, J.C. (2005b), "Structural damage diagnosis under varying environmental conditions-part II: Local PCA for non-linear cases", *Mech. Syst. Signal Pr.*, **19**, 865-880.

Yu, L. and Zhu, J.H. (2015), "Nonlinear damage detection using higher statistical moments of structural responses", *Struct. Eng. Mech.*, **54**(2), 221-237.

PL